water

MDPI

Article

Influence of Vegetation Coverage on Hydraulic Characteristics of Overland Flow

Zekang Cai [1], Jian Wang [1,*], Yushuo Yang [2] and Ran Zhang [1]

[1] College of Natural Resources and Environment, Northwest Agriculture and Forestry University, Yangling, Shaanxi 712100, China; Zekang00@163.com (Z.C.); 909423488@nwafu.edu.cn (R.Z.)
[2] College of Landscape Architecture and Art, Northwest Agriculture and Forestry University, Yangling, Shaanxi 712100, China; 2018011457@nwafu.edu.cn
* Correspondence: wangjian@nwafu.edu.cn; Tel.: +86-13-909-248-519

Abstract: Soil erosion is a major problem in the Loess Plateau (China); however, it can be alleviated through vegetation restoration. In this study, the overland flow on a slope during soil erosion was experimentally simulated using artificial grass as vegetation cover. Nine degrees of vegetation coverage and seven flow rates were tested in combinations along a 12° slope gradient. As the coverage degree increased, the water depth of the overland flow increased, but the flow velocity decreased. The resistance coefficient increased with increasing degree of coverage, especially after a certain point. The resistance coefficient and the Reynolds number had an inverse relationship. When the Reynolds number was relatively small, the resistance coefficient decreased faster; however, when it exceeded 600, the resistance coefficient decreased at a slower rate. A critical degree of vegetation cover was observed in the relationship between the resistance coefficient and submergence degree. When the degree of coverage was greater than 66.42%, the resistance coefficient first decreased and then increased with a higher submergence degree. Finally, the formula for the resistance coefficient under vegetation coverage was derived. This formula has a relatively high accuracy and can serve as a reference for predicting soil erosion.

Keywords: vegetation cover; overland flow; hydraulic characteristics; resistance mechanism

Citation: Cai, Z.; Wang, J.; Yang, Y.; Zhang, R. Influence of Vegetation Coverage on Hydraulic Characteristics of Overland Flow. *Water* **2021**, *13*, 1055. https://doi.org/10.3390/w13081055

Academic Editor: Achim A. Beylich

Received: 11 March 2021
Accepted: 8 April 2021
Published: 12 April 2021

1. Introduction

The Loess Plateau in China is situated in the arid continental monsoon climate zone; it experiences concentrated rainstorms and has a loose soil structure. Thus, it is an area that suffers from serious soil erosion as well as soil and water loss [1]. However, improvements in vegetation coverage in recent years have helped ameliorate erosion losses to a certain extent [2]. In 1999, the vegetation coverage of the Loess Plateau was 32%, but it has since increased to 59%. The vegetation coverage in northern Shaanxi, which suffers from severe soil erosion, has also increased significantly. The vegetation coverage reached 81% in 2017, and the forest coverage reached 46% [3]. Vegetation is an essential component of the ecosystem in the region, it intercepts rainfall and runoff, and blocks and stabilizes sand [4,5]. Vegetation can have a significant effect on hydrological fluxes due to variations in the physical characteristics of the land surface, soil, and vegetation; such as the roughness, albedo, infiltration capacity, root depth, architectural resistance, leaf area index (LAI), and stomatal conductance [6].

The most effective and economical means of ecological restoration is to plant vegetation on the slopes to prevent and control soil erosion [7]. Since 2000, owing to promulgation of the policy of returning farmland to forests, the vegetation coverage of the Loess Plateau has significantly increased. In addition, soil erosion in this area has been greatly reduced.

To explore the role and mechanism of the vegetation measures during the flow and sediment reduction process, as well as to investigate the impact of vegetation coverage on the hydrodynamic characteristics of overland flow, researchers worldwide have conducted numerous simulation experiments [8–10]. These simulation experiments have laid down the theoretical basis for soil erosion research. The flow regime of overland flow has always been the research focus of domestic and foreign researchers, who have put forward many different points of view. Selby [11] indicated that the overland flow is a mixture of turbulent and laminar flows. Pute and Peihua [12] indicated that the overland flow is a special and complicated type of laminar flow. They stated that this is because of its appearance, which exhibits ripples that converge from many small streams, which they referred to as "agitated laminar flow." Horton [13] stated that overland flow is in a mixed state, that is, a completely turbulent flow zone that is interspersed with laminar flow zones. Zhang [14] demonstrated the critical hydraulic conditions for the turbulent state of shallow overland sheet flow. In other words, when the water depth is less than 0.316 cm, the water flow is transitional; when the water depth is greater than 0.347 cm, the water flow is in a turbulent state. Wu et al. [15] reported that overland flow under the soil crust is laminar. Pan and Shangguan [16] proposed that under the influence of grass coverage, the flow regimes of overland flow are distributed into laminar and tranquil flow zones. Regarding the nature of the flow regime of overland flow, there are many divergent opinions; thus, this is a problem worth exploring. The flow velocity is also an important factor that influences slope erosion, which is related to the degree of vegetation coverage, flow rate, and slope gradient. In the absence of vegetation coverage, it is generally believed that the flow rate is the dominant factor that influences flow velocity [14]. Cao et al. [17] reported that the degree of grass coverage has a greater impact on flow velocity than slope gradient or flow rate; however, the study by Abrahams et al. [10] demonstrated that flow rate plays a more significant role with regard to flow velocity than surface roughness or slope gradient.

The overland flow resistance is an important factor that influences soil erosion as well as water and soil loss. It is affected by the degree of vegetation coverage, species of vegetation, surface roughness, and many other factors [18,19]. However, the influence of factors on slope resistance is very complex. Since the 1970s, several researchers have carried out a large number of studies on overland flow resistance [20]. Studies by Zhang et al. [21] and Smith [22] demonstrated that the resistance coefficient exhibits a decreasing trend with increases in the Reynolds number [23,24]. Chen and Yao [25] showed that the resistance coefficient of uniform overland flow is related to the bed surface roughness in the laminar flow and smooth zones of the turbulent flow. In addition, the slope gradient also affects the resistance coefficient of uniform overland flow. Regarding the resistance under vegetation coverage, it is generally believed that the resistance effects caused by the various resistance forms are linearly superimposed [26]. However, Li [27] obtained different results. When considering the many studies that have investigated the resistance mechanisms, it is observed that the test conditions often differ substantially from the actual situation. Despite the numerous research results worldwide, the mechanisms and influencing factors of overland flow resistance remain unclear; thus, further research is needed in this regard.

As an important tool to analyze hydrological processes, hydrological models have been very useful for analyzing the influence mechanism of soil hydrological attributes on hydrological processes, which is an important research issue in hydrology [28,29]. The influence mechanism of soil hydrological properties on hydrological processes at different scales is also a frontier of hydrological research. Paul et al. proposed and successfully implemented a modified time variant SDDH method in a routing module. Their test results showed that the modified cell-to-cell routing scheme performed better than the original physically based method [30]. The Variable Infiltration Capacity (VIC) model has also been adopted to analyze the effects of uniform and heterogeneous agricultural land use over the hydrological responses of the basin by changing crop-specific vegetation parameters [6]. However, the hydrological processes under vegetation cover are relatively complex, and the models and formulas in this area need to be further explored [31,32].

Thus, in this study, combinations of nine degrees of vegetation coverage and seven flows were tested with a 12° slope gradient by using artificial grass to simulate the slope vegetation coverage. The purpose of this research study was to (1) explore the changing patterns of the hydraulic parameters of overland flow; (2) quantify the impact of degree of vegetation coverage on the overland flow resistance; and (3) establish a formula for the resistance coefficient under a given vegetation coverage condition. This study reveals the general trend of hydraulic parameters under various degrees of vegetation coverage. The research results can serve as a reference for predicting slope erosion when implementing water and soil conservation measures.

2. Materials and Methods

2.1. Experimental Design

This experiment was conducted in a rectangular variable-slope flume made of Plexiglas® (Figure 1). The dimensions of the flume were 4.5 m × 0.3 m × 0.25 m (length × width × height). A 40-grit water sandpaper was placed on the bottom of the flume to simulate slope surface roughness and to ensure stability of the underlying surface during the test. Starting from the flume entrance, the 1-m upstream section represents a bare slope, and the 3-m middle section represents a slope covered with vegetation. A total of seven observation sections (one in the upstream of the vegetation section, five in the vegetation section, and one in the downstream) were arranged. All the observation sections were equipped with two ultrasonic water level sensors (Sinomeasure SIN-DP, Hangzhou China).

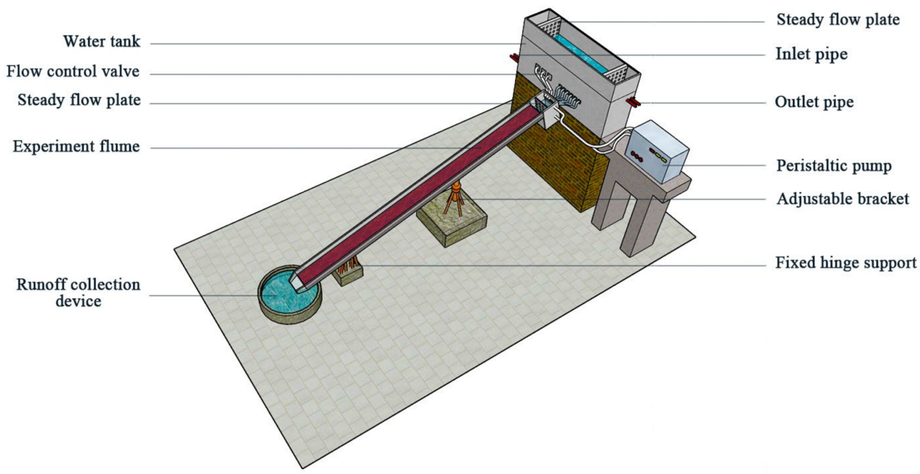

Figure 1. Test device (the device was developed and setup by the authors in Key Laboratory of Agricultural Soil and Water Engineering of the Ministry of Education in Arid Areas).

Artificial grass of the clustered needle-shape type was chosen to simulate the vegetation cover on the slope; 50 grass leaves with a diameter of approximately 1 mm were fixed on the base surface with a 2 cm diameter to form a cluster of artificial grass, which was approximately 20 mm in height. The spatial arrangement of the grass followed a random patch distribution.

The vegetation densities used in this study were 9.76%, 19.97%, 38.78%, 47.66%, 66.42%, 76.73%, 85.72%, and 95.01% (Figure 2). After analyzing the terrain and slope data of the Loess Plateau region, the slope of the flume was selected to be 12° [25,33]. By considering the critical rainfall intensity that induces soil erosion and the ranges of the hydrodynamic conditions [34,35], the unit discharge was designed to increase from 0.000278 m^2/s to 0.00167 m^2/s in this test.

In Table 1, the vegetation coverage density was calculated by dividing the cross-sectional area of the grass stems by the area of the plot; the corresponding calculation formula is as follows:

$$Cr = \frac{n\pi r^2}{BL} \quad (1)$$

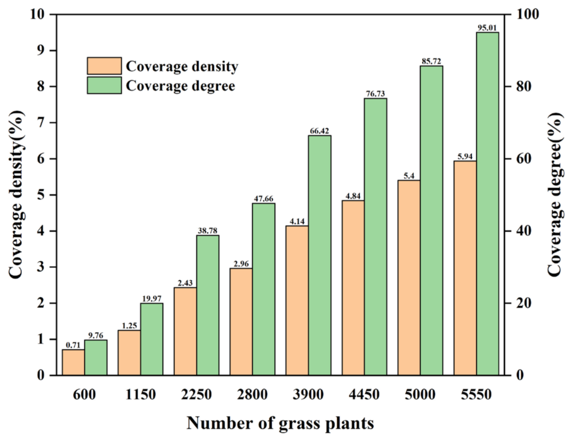

Figure 2. Vegetation coverage density and degree vs. number of grass plants used in this test.

Table 1. Ranges of hydraulic parameters for different degrees of vegetation coverage.

Coverage Treatment (%)	Unit Discharge (m^2/s)	Water Depth (mm)	Flow Velocity (m/s)	Reynolds Number	Froude Number	Resistance Coefficient
0	0.000278–0.00167	1.65–3.73	0.168–0.447	243.38–1460.31	1.32–2.34	0.30–0.95
9.76	0.000278–0.00167	1.76–4.22	0.158–0.395	243.38–1460.31	1.20–1.94	0.44–1.15
19.97	0.000278–0.00167	1.80–4.41	0.154–0.378	243.38–1460.31	1.16–1.80	0.50–1.23
38.78	0.000278–0.00167	1.83–4.70	0.152–0.355	243.38–1460.31	1.13–1.65	0.61–1.30
47.66	0.000278–0.00167	1.94–4.71	0.143–0.354	243.38–1460.31	1.03–1.64	0.61–1.54
66.42	0.000278–0.00167	1.97–6.01	0.141–0.277	243.38–1460.31	1.01–1.14	1.23–1.62
76.73	0.000278–0.00167	2.22–6.79	0.125–0.245	243.38–1460.31	0.84–0.95	1.84–2.31
85.72	0.000278–0.00167	2.37–7.44	0.117–0.224	243.38–1460.31	0.77–0.83	2.42–2.82
95.01	0.000278–0.00167	2.65–8.11	0.105–0.206	243.38–1460.31	0.65–0.73	3.13–3.94

The coverage can be calculated by dividing the projected area of the vegetation canopy by the area of the test region. The parameters for the above formula are as follows: Cr is the degree of vegetation coverage; n is the total number of grass stems; r is the radius of the grass stem, in mm; L is the length of the test section, in m; and B is the flume width, in m.

In the measurement method, the ultrasonic water level needle gauges (Sinomeasure SIN-DP, Hangzhou, China) were used to measure the water depth, and the surface velocity radar (Sirius Flow tar-SVR, Stroudsburg, PA, USA) was used to measure the surface velocity of the water flow based on the potassium permanganate dye tracer (Figure 3).

(**a**) (**b**)

Figure 3. Flow velocity measurement using potassium permanganate (**a**) at the start of the experiment and (**b**) after 0.79 s.

2.2. Simulation Accuracy Evaluation Method

2.2.1. Nash–Sutcliffe Efficiency

The Nash–Sutcliffe efficiency (*NSE*) is generally used to verify the quality of hydrological model simulation results. The value of *NSE* ranges from negative infinity to one. An *NSE* close to one indicates a good-quality model with high reliability, whereas an *NSE* close to zero indicates that the simulation result is close to the average of the measured values. In other words, the overall result is credible, but the process simulation error is large. However, when the *NSE* is far below zero, it is considered that the model is not credible. The corresponding equation is as follows:

$$NSE = 1 - \frac{\sum_{i=1}^{n} (O_i - P_i)^2}{\sum_{i=1}^{n} (O_i - \overline{O})^2} \tag{2}$$

where P_i is the sample's simulated value, O_i is the sample's measured value, $\overline{O}$ is the average of the sample's measured values, and n is the number of samples.

2.2.2. Regression Analysis

R^2 reflects the goodness-of-fit of the regression equation, which can be used to determine the fitting quality of the regression. If its value is close to one, the fitting effect is good; otherwise, the fitting effect is poor. The corresponding equation is as follows:

$$R^2 = \frac{SSR}{SST} \tag{3}$$

where $SSR = \sum(\hat{y}_i - \overline{y})^2$ is the explained sum of squares (ESS), $SST = \sum(y_i - \overline{y})^2$ is the residual sum of squares (RSS), y_i is the calculated resistance of the ith group, $\overline{y}$ is the calculated average resistance, and $\hat{y}_i$ is the fitted resistance of the ith group.

2.2.3. Root Mean Square Error

Root mean square error (*RMSE*) represents the standard deviation of the difference between the predicted and observed values, and has been widely used to quantify the accuracy of a measurement. The closer this value is to zero, the more accurate the measurement is. It can be calculated using the following equation:

$$RMSE = \sqrt{\frac{1}{n}\sum_{i=1}^{n}(f_i - y_i)^2} \tag{4}$$

where f_i is the predicted value of the sample, y_i is its observed value, and n is the number of samples.

2.2.4. Mean Absolute Error

Mean absolute error (MAE) represents the mean of the absolute error between the predicted value and the observed value. Its calculation formula is as follows:

$$MAE = \frac{1}{n}\sum_{i=1}^{n}|f_i - y_i| \tag{5}$$

3. Results

3.1. Hydraulic Parameters under Various Degrees of Vegetation Coverage

Table 1 summarizes the ranges of the water depth, flow velocity, Reynolds number, Froude number, and other hydraulic parameters recorded under different underlying surface conditions in this experiment.

It can be observed from the table that overland flow water depth is affected by variation in the unit discharge and the degree of vegetation coverage. As the unit discharge increases from 0.000278 m^2/s to 0.00167 m^2/s, overland flow water depth under vegetation cover can reach depths of up to 8.11 mm, and the depth values are all higher than those without vegetation cover. As the vegetation coverage increases, the average water flow velocity slows down. On the bare slope, the flow velocity is between 0.168 and 0.447 m/s; when the degree of coverage is 9.76%, the flow velocity decreases to 0.158–0.395 m/s; and when the degree of coverage increases to 95.01%, the flow velocity can drop to 0.105–0.206 m/s. In addition, the range of Reynolds number under vegetation cover is 243.38–1460.31. It is observed that the Froude number decreases with an increase in the degree of vegetation coverage, from 1.32–2.34 (without vegetation cover) to 0.65–0.73.

3.2. *Influence of Vegetation Coverage on Water Path and Flow Velocity*

Figure 4 indicates that overland flow water depth increases with the degree of coverage, and also surges with increases in the flow rate. In the coverage range of 9.76% to 47.66%, the water depth exhibits only a slight increase; however, when the degree of coverage exceeds 47.66%, the water depth shows a dramatic increase. For example, when the flow rate is 0.33 L/s, the water depth rises from 3.03 mm to 7.29 mm with an increase in the degree of coverage; when the flow rate is 0.50 L/s, the water depth increases from 3.73 mm to 8.11 mm. This is possible because the vegetation has a relatively small blocking effect on the water flow at a low degree of coverage. In addition, when considering a 12° slope gradient, the energy generated by the gravity component of the water flow along the slope is relatively large. As a result, the degree of vegetation coverage has a relatively small impact on overland water flow. As the degree of coverage increases, both the vegetation coverage area and the effective area rapidly increase, the discharge area decreases, and the backwater increases, thus resulting in an increase in the measured water depth.

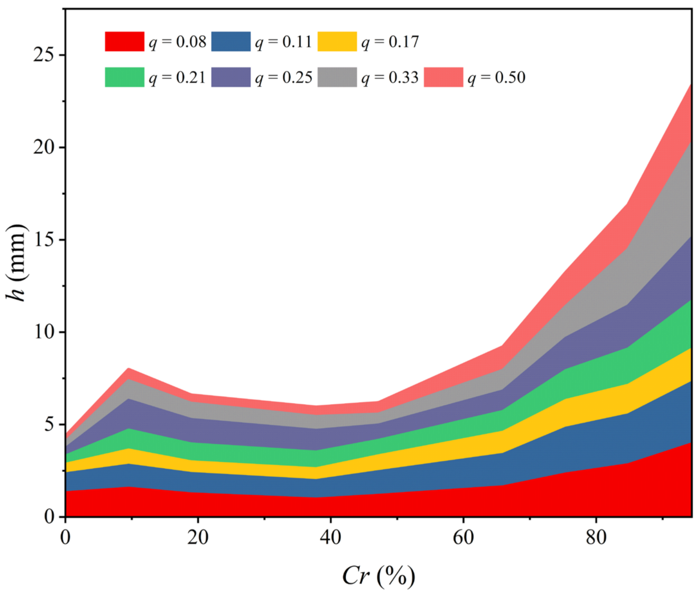

Figure 4. Relationship between water depth (h) and degree of coverage (Cr).

Figure 5 indicates that under vegetation cover, flow velocity increases with increasing flow rate. In this experiment, under a fixed 12° slope gradient and a constant flow rate, overland flow velocity exhibited an overall downward trend with an increase in the degree of coverage. For example, when the flow rate is 0.33 L/s, overland flow velocity reduces from 0.367 m/s to 0.313 m/s under 9.76% vegetation coverage; when the flow rate is 0.5 L/s, overland flow reduces from 0.447 m/s to 0.395 m/s under 9.76% vegetation coverage. This shows that the variation of the degree of vegetation coverage has a significant impact on the hydrodynamic parameters of the water flow.

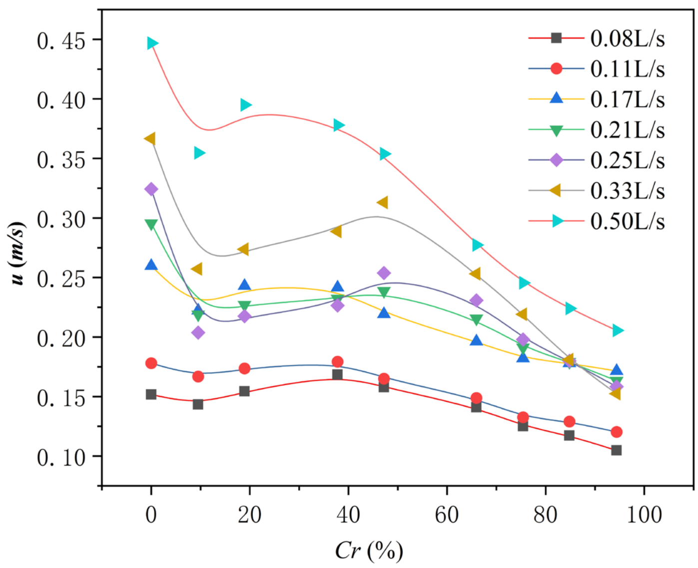

Figure 5. Relationship between mean velocity (*u*) and degree of coverage (*Cr*).

3.3. Relationship between Darcy Resistance Coefficient and Vegetation Coverage

Figure 6 shows the relationship between the Darcy resistance coefficient and the degree of vegetation coverage. When there is vegetation cover, the Darcy resistance coefficient is higher than that without vegetation. In addition, the resistance coefficient increases continuously with increase in the degree of coverage. However, the vegetation coverage does not show a prominent increase in the resistance effect. When the degree of coverage is between 47.66% and 95.01%, the overland flow resistance coefficient increases rapidly with increases in the degree of coverage. For example, when the degree of coverage is 66.42%, the resistance coefficient is in the range of 1.23–1.62. When the coverage is 87.72%, the resistance coefficient is in the range of 2.42–2.82, which is nearly double.

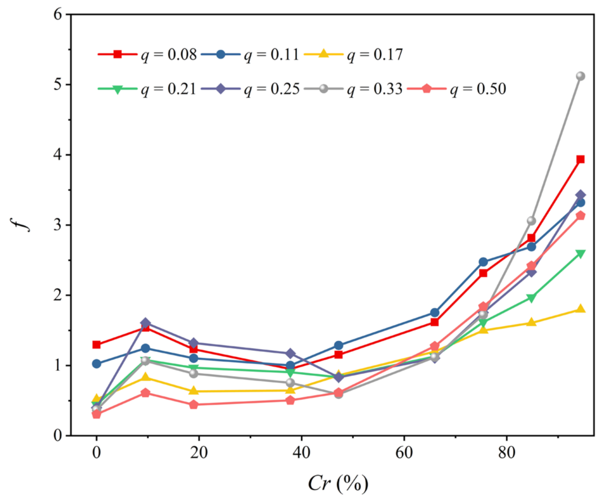

Figure 6. Relationship between resistance coefficient (*f*) and degree of coverage (*Cr*).

3.4. Relationship between Manning Coefficient and Vegetation Coverage

For natural rivers, the Manning roughness coefficient in the Manning formula is often used to characterize the roughness of the river. For overland flow, this value reflects the influence of the underlying surface factors on the flow of water. Figure 7 shows the relationship between the degree of vegetation coverage and the roughness coefficient.

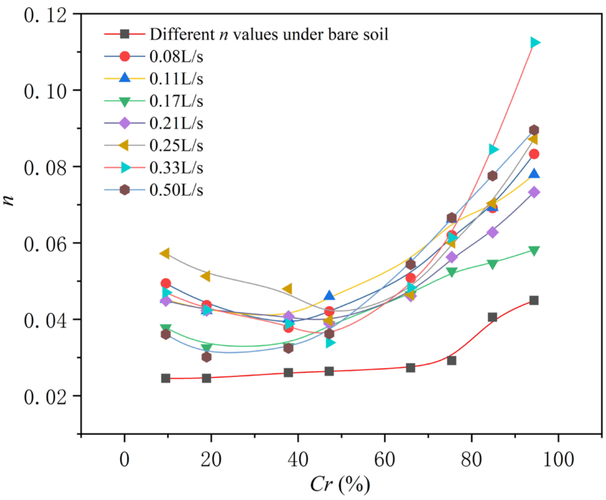

Figure 7. Relationship between vegetation coverage (*Cr*) and roughness coefficient (*n*).

Under all the conditions, the roughness coefficients under vegetation cover are all higher than those without vegetation. The Manning roughness coefficient for the bare slope is in the range of 0.025–0.038; when the degree of coverage is 9.76%, the roughness coefficient is in the range of 0.030–0.042, and the roughness increases with increasing degree of vegetation coverage. When the degree of coverage is below 47.66%, this increasing trend is not obvious. However, when the degree of coverage is greater than 47.66%, the roughness coefficient increases linearly with an increase in the degree of coverage. For example, when the degree of coverage is 66.42%, the roughness coefficient is in the range of 0.051–0.054; when the degree of coverage is 85.72%, the roughness coefficient is in the range of 0.083–0.112, which is an increase of nearly 1.5 times. It can also be observed that when the degree of vegetation coverage is low, the roughness is not significantly affected by the flow rate, and its value varies only within a small range with the flow rate. When the degree of vegetation coverage becomes higher, the data points in the figure become more dispersed with the flow rate. When the slope gradient is 12° and the degree of coverage reaches 76.73%, the roughness coefficient is affected more by the flow rate.

3.5. Analysis of Darcy Resistance Coefficient

3.5.1. Relationship between Darcy Resistance Coefficient and Reynolds Number

The relationship between the Reynolds number and the resistance coefficient is affected by the vegetation density. Researchers [3,36–38] have demonstrated that the resistance coefficient is mainly related to the Reynolds number, and the two parameters exhibit different variation patterns under different vegetation densities, as shown in Figure 8.

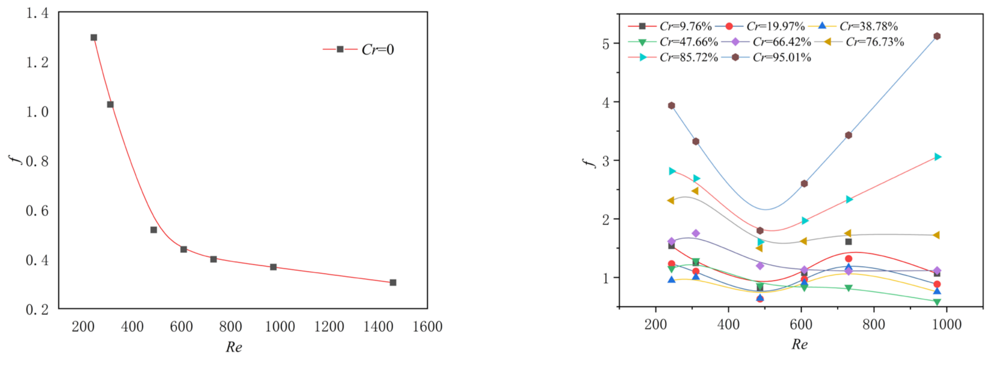

(**a**) (**b**)

Figure 8. Relationship between resistance coefficient (*f*) and Reynolds number (*Re*): (**a**) without vegetation cover; (**b**) with vegetation cover.

When the surface has no vegetation cover, the resistance coefficient and the Reynolds number have an inverse relationship. When the Reynolds number is small, the resistance coefficient decreases at a faster rate; however, when the Reynolds number exceeds 600, the resistance coefficient decreases at a slower rate. This is possible because by having a low Reynolds number, the flow rate and water depth of overland flow are both relatively small. When the slope gradient is steep, the instability of the water flow is very evident. In addition to the grain resistance of the bed surface, the wave resistance generated by the rolling wave is also an important component of the total resistance and it has a significant impact on the total resistance coefficient. Therefore, the variation in the resistance coefficient is large. However, at a high Reynolds number, the water depth is relatively deep, the water flow tends to be stable, and the generated wave resistance no longer has an obvious effect on the total resistance. It can be observed from Figure 8b that when the degree of coverage is 66.42% in the boundary, the resistance coefficient exhibits an overall decreasing trend with increase in the Reynolds number when the vegetation coverage is below this critical value. When the degree of vegetation coverage exceeds this critical value, the resistance coefficient decreases with increase in the Reynolds number in the laminar flow zone; however, when the water flow gradually develops to the transitional flow zone, the resistance coefficient under a high degree of coverage continues to increase with increase in the Reynolds number. For example, when the degree of coverage is 47.66%, the resistance coefficient reduces from 1.296 to 0.610 when the water flow develops from the laminar flow zone to the transitional flow zone. When the degree of coverage is 85.72%, in the laminar flow zone, the resistance coefficient reduces from 2.815 to 1.969, and then it gradually increases to 3.059 with an increase in the Reynolds number. This is possible because when the water flow on the vegetation-covered slope is distributed in the laminar flow zone, the water depth is very shallow, and the slope resistance is dominated by grain resistance. However, in the transitional flow zone, the turbulence intensity of the water flow is high, and the backwater phenomenon is more obvious. Vegetation with a high degree of coverage exhibits a better blocking effect on the water flow and it increases the flow resistance.

3.5.2. Relationship between Darcy Resistance Coefficient and Submergence Degree

Figure 9 shows the relationship between the resistance coefficient and the submergence degree. The submergence degree of the vegetation cover can affect the velocity distribution [39] of overland flow. It also has a certain impact on the hydrodynamic parameters of overland flow [38].

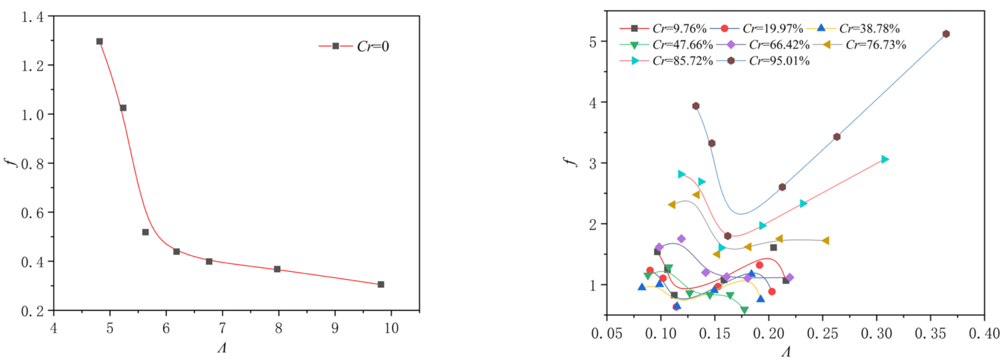

(**a**) (**b**)

Figure 9. Relationship between resistance coefficient (f) and submergence degree (Λ): (**a**) without vegetation cover; (**b**) with vegetation cover.

Figure 9a indicates that when there is no vegetation cover, the submergence degree is greater than one. In this case, the Darcy resistance coefficient and the submergence degree have an inverse relationship, and its changing trend is similar to what is observed between the Darcy resistance coefficient and Reynolds number for the bare slope. It can be observed from Figure 9b that under vegetation cover, the submergence degree is less than one. In addition, there is a critical degree of vegetation coverage in the relationship between the resistance coefficient and submergence degree. When the degree of coverage is below 66.42%, the resistance coefficient exhibits an overall decreasing trend with increase in the submergence degree. When the degree of coverage is greater than this critical value, as the submergence degree increases, the resistance coefficient first rapidly decreases and then it continues to increase. When the degree of coverage is 95.01%, the resistance coefficient drops from 3.935 to 2.602, and then it increases to 5.120. This phenomenon is related to the ratios of grain resistance and vegetation resistance that were previously mentioned.

3.5.3. Influence of Flow Rate and Degree of Coverage on Ratio of Form Resistance

Figure 10 shows the influence of flow rate and degree of coverage on the ratio of form resistance. Under the different vegetation coverage conditions, the contribution of form resistance to the total resistance is significantly different. Form resistance is expressed as follows:

$$f_{form} = f_{total} - f_{grain} \tag{6}$$

where f_{form} is the form resistance, f_{total} is the total resistance, and f_{grain} is the grain resistance. Grain resistance level can be represented by the resistance under the bare slope condition. The ratio of form resistance can be expressed by ∂, and it can be determined as follows:

$$\partial = \frac{f_{form}}{f_{total}} \tag{7}$$

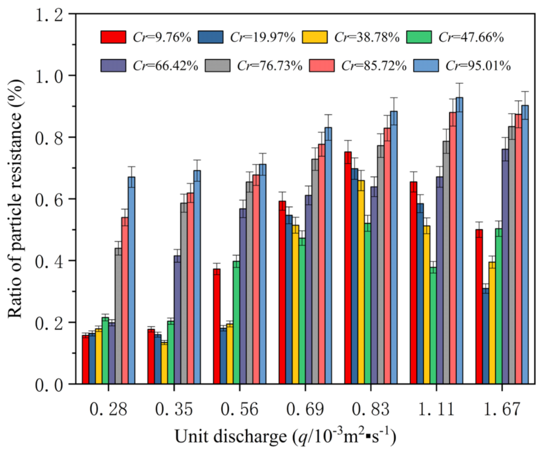

Figure 10. Relationship between ratio of particle resistance and unit discharge.

When the degree of vegetation coverage is relatively low, the ratio of form resistance first increases and then decreases with the flow rate. The critical degree of coverage corresponding to the maximum form resistance is 66.42%. For example, when the degree of vegetation coverage is 9.76%, as the unit discharge increases from 0.00028 m^2/s to 0.00083 m^2/s, the ratio of form resistance increases from 0.176 to 0.521; however, as the flow rate continues to increase to 0.00167 m^2/s, form resistance gradually drops to 0.309. When the degree of vegetation coverage is relatively high, the ratio of form resistance in the total water flow resistance increases with an increase in the flow rate, and the rate of increase gradually decreases with an increase in the density. For example, when the degree of vegetation coverage is 85.72%, as the unit discharge increases from 0.00028 to 0.00167 m^2/s, the ratio of form resistance gradually increases from 0.663 to 0.874, which shows an increase of 0.211. However, when the degree of coverage is 95.01%, within the same range of flow rate, the ratio of form resistance increases from 0.758 to 0.903, which represents an increase of only 0.145.

3.6. Empirical Formula for Resistance Coefficient

Analysis of the experimental data indicates that vegetation density is also an important parameter that affects the resistance coefficient. Overland flow patterns under different vegetation densities will differ from one to another. To establish a resistance coefficient formula that conforms to the vegetation coverage conditions, the influence of the variations in vegetation density *Cr* on the total resistance is considered, and the vegetation density is introduced as the fitting parameter of the resistance formula (Figure 11) (Appendix A).

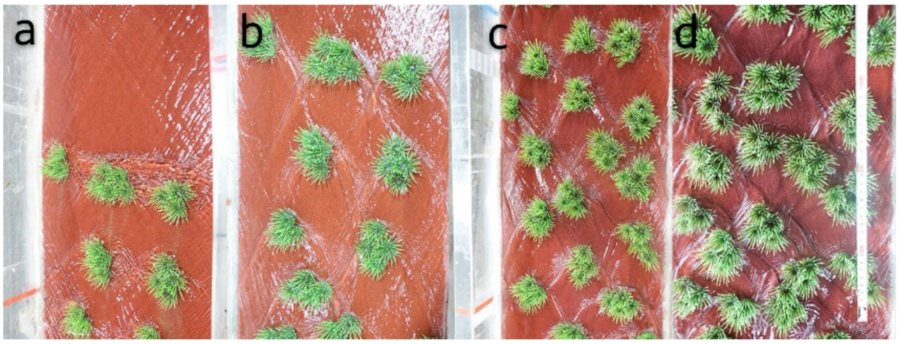

Figure 11. The process of vegetation being submerged for (**a**) 9.76%, (**b**) 19.97%, (**c**) 47.66%, and (**d**) 66.42% vegetation coverage.

By being directly derived from the nonlinear regression, the analysis results of the experimental data show that the degree of coverage *Cr*, the Reynolds number *Re*, and the unit discharge q are all highly correlated with the resistance coefficient. As *Cr* cannot be zero, the equivalent discharge area (1 – *Cr*) is chosen as the parameter. From the resistance coefficient graph, the basic formula for f is as follows:

$$f = k(1 - Cr)^{a} Re^{b} q^{d} \quad (8)$$

According to the multiple nonlinear regression analysis on the test data (using IBM SPSS Statistics 20.0), the following expression was determined:

$$f = 0.560(1 - Cr)^{-31.71} Re^{-0.049} q^{-0.017}, \ \left(R^2 = 0.747\right). \quad (9)$$

4. Discussion

4.1. Experimental Phenomena during Vegetation Submergence

Figure 11a–d show the overland flows on slopes with various vegetation-cover densities. It can be observed that the presence of vegetation cover can affect the movement of overland flow. In other words, the vegetation cover has changed the discharge area of overland flow. When the flow rate is relatively small, the water depth is very shallow. In this case, the vegetation cover has little impact on the water flow, and the flow regime does not change significantly. As the water depth increases, the presence of vegetation can significantly hinder the water flow and force it to change its path of movement. A small part of the water flow passes through the vegetation, while the majority flows through the gap between the vegetation (i.e., the flow-around phenomenon), which reduces the discharge area and results in backwater in the vegetation-covered areas. When the vegetation density increases to a certain level and the water level is relatively high, the vegetation's blocking effect and the disturbance of the water flow will be more severe, thus slowing down the flow velocity.

4.2. Influence of Vegetation Coverage on Water Depth and Flow Velocity

Figure 5 illustrates that the flow velocity increases with increases in the flow rate under vegetation cover, but it decreases with increases in the degree of coverage. When the degree of coverage is between 9.76% and 47.66%, the flow velocity increases with the degree of vegetation coverage, and the decreasing trend is not obvious. In this case, the water flow has been in contact with the vegetation during its flow process. However, because of the large flow velocity gradient on a steep slope, the intensity and potential energy of the water flow are relatively high, which results in a relatively small change in overland flow velocity.

In this range of vegetation coverage, fluctuations in the velocity change can be observed, which may be because of the uneven flow velocity distribution that is parallel to the slope caused by the distributed vegetation during the velocity measurement. In addition, under the vegetation cover conditions, the water flow can be easily blocked during its flow process; thus, resulting in instabilities in the measured values. When the degree of coverage is greater than 47.66%, the flow velocity drops rapidly. This means that above this critical degree of coverage, the water flow is affected more by the vegetation than the slope gradient. The slope gradient of the primary ecological hydraulic erosion zone of the Loess Plateau is generally below 10°, which is dominated by splash erosion and sheet erosion. The slope gradient of the rill and shallow gully erosion is generally between 10° and 35°. Therefore, to improve the effectiveness of the vegetation coverage measures in practice, a degree of coverage that is greater than 47.66% can be used as a valid reference.

4.3. Flow Regime of Overland Flow under Vegetation Cover

Figure 12 shows the flow regime of overland flow under vegetation cover. Most of the data points are distributed in the torrent laminar flow zone and the torrent transitional flow zone. A small number of data points are distributed in the slow laminar flow zone and the slow transitional flow zone; no data points reach the turbulent flow zone.

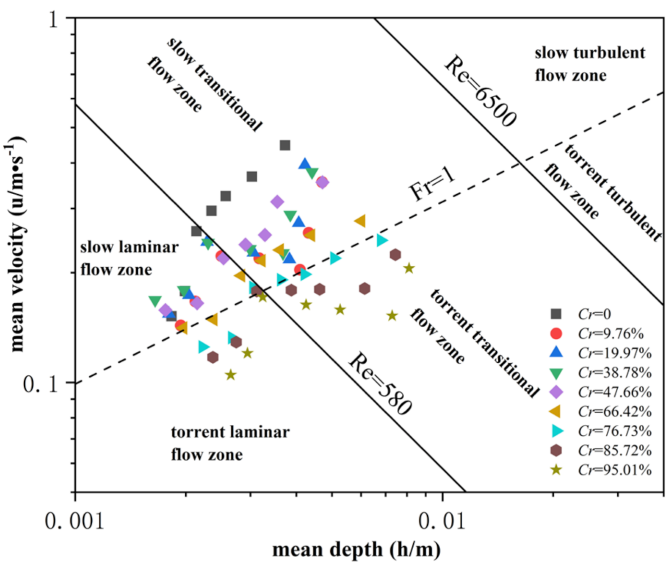

Figure 12. Flow regime under different degrees of vegetation coverage.

Figure 12 indicates that overland flow under vegetation cover is in the mixed flow zone of the laminar and transitional flows. This result is similar to the case when there is no vegetation cover. Therefore, the presence of vegetation cover does not significantly change the flow zone distribution of overland flow. From a comprehensive consideration of the relationship between the flow velocity and water depth, it was demonstrated that overland flow under the vegetation cover is in the mixed flow zone of the laminar and transitional flows, which is similar to the test results that were observed in the absence of the vegetation cover. Zhang et al. [40] described the laminar flow zone in this phenomenon as a "virtual laminar flow zone." They believe that the open-channel flow hydraulics can no longer meet the needs of overland flow research in this case. There are certain limitations in simply using the criterion of a Reynolds number that is below 580 to demonstrate that the water flow is in the laminar flow zone as it does not conform to the actual situation. In particular, when the degree of coverage is high, the water flow is significantly disturbed by the vegetation cover, and it cannot spread out and flow evenly on the flume bottom. Instead, it will gather into streams and flow through the vegetation. On the upstream face of each grass plant, a backwater depth will be generated. Meanwhile, on the downstream face, the stream will be disconnected, and a wake vortex will appear. The near-wall flow around the plant will only occur under a very large flow rate or a very small energy slope. When the coverage increases, the backwater from the upstream face of the vegetation gets progressively closer, and the waves blend into the water flow and eventually become rolling waves. In this study, when the flow rate was small, the free surface of the water flow became unstable and presented wavy movement. If the flow rate continued to increase, the rolling wave would gradually fade and the water surface would return to balance. This occurred because the destruction effect of the water inertia force is greater than the balance effect of the viscous force, which promotes the flow to a new balance and makes the overall flow smooth by sacrificing some fluid particles. This is also the reason why the overland flow in this test is in the mixed flow zone.

Researchers have tried different characteristic lengths to calculate the Reynolds number of overland flow. For example, for the open channels with vegetation cover, the water depth [41], plant diameter [42], or vegetation spacing [43] (Table 2) are used as the characteristic lengths. The results show that under a low degree of vegetation coverage, the turbulence intensity is relatively low, the resistance energy consumption is also low, and the flow velocity is the dominant form of energy conversion. The results also show that under a low degree of coverage, the vertical distribution gradient of the flow velocity is relatively large. However, as the degree of vegetation coverage increases, the collision probability of the water flow and the roughness factor increases, and the mixing probability of the flow layers also increases; thus, making the vertical flow velocity distribution more uniform.

Table 2. Summary of studies that collected different characteristic lengths and Reynolds numbers.

Study	Characteristic Lengths	Reynolds Number
Wu et al. 1999	Normalized flow depth (D/T) a) Unsubmerged vegetation D/T = 0.6–1.0; b) submerged vegetation D/T = 1.0–7.4	20–3000
Ishikawa et al. 2000	Solid volume fraction (Φ) Laboratory measurements are presented for Φ = 0.091 (Square); Φ = 0.15 (Left triangle); Φ = 0.20 (Cross); Φ = 0.27 (Hexagram); Φ = 0.35 (Circle)	25–685
Tanino and Nepf 2008	Diameter of model tree (d) Model trees with different diameters (0.40 and 0.64) were used to set two different spacing (6.32 and 3.16) for comparison	<5000

In regard to the flow regime of the water flow, when the degree of coverage increases from 0% to 95.01%, the water flow shifts away from the torrent flow zone and it gradually approaches the slow flow zone. When the degree of vegetation coverage reaches 76.73%, the overland water flow is almost completely in the torrent flow zone. This observation is consistent with the research results obtained by Dunkerley et al. [44], Yi and Ming'an [45], and Wu et al. [46]. In other words, for overland flow under vegetation cover, the effect of the vegetation cover is enhanced and that of the turbulence of the water flow is reduced. This phenomenon can be attributed to the influence of the vegetation's resistance. As the degree of coverage increases, the water blocking surface area of the vegetation increases continuously, thus leading to an increase in the drag force on the overland water flow. This drag force is positively proportional to the square of the flow velocity. Therefore, for water flows under large coverage conditions, the increase in the resistance plays a dominant role, which results in a decrease in flow rate and Froude number.

4.4. Resistance Generation Mechanism under Different Degrees of Vegetation Coverage

Figure 6 shows that the resistance coefficient continues to increase with the increase in the degree of coverage; however, when the degree of coverage is 47.66%, which occurs in the boundary, this changing trend becomes obvious. This is possible because when the degree of coverage is low, the effective contact area between the vegetation and water flow is relatively small. In this case, the vegetation resistance only accounts for a small proportion of the total resistance, and the resistance coefficient is not greatly affected by the degree of coverage. This is because grain resistance and sidewall resistance are the dominant components in the total resistance under a low degree of coverage, and the impact of the vegetation coverage on the water flow is not significant.

In Figure 8, when the degree of vegetation coverage is less than 66.42%, the resistance coefficient exhibits an overall decreasing trend as the Reynolds number increases. When the degree of vegetation coverage is greater than this critical value, the resistance coefficient decreases with an increase in the Reynolds number in the laminar flow zone. However, as the water flow gradually develops into the transitional flow zone, the resistance coefficient under a large degree of coverage also continues to increase with an increase in the Reynolds number. This is possible because when the water flow on the vegetation-covered slope is distributed in the laminar flow zone, the water depth is very shallow, and the slope resistance is dominated by the grain resistance. However, when the vegetation coverage is small, the kinetic energy resulting from the increase in the flow offset the obstructing effect of the vegetation, and the proportion of the grass cover morphological resistance does not increase significantly. Further, when the vegetation coverage continues to increase, in the transition flow zone, the turbulence intensity of the water flow is high, and the backwater phenomenon becomes more obvious. The vegetation cover with a high degree of coverage exhibits a better blocking effect on the water flow and it increases the water flow resistance. Figures 8b and 9b show the rapid increase in the resistance coefficient with the high coverage rate.

An analysis of Figure 10 indicates that at a relatively low degree of vegetation coverage, the ratio of form resistance in the total water flow resistance first increases and then decreases with increasing flow rate. When the degree of vegetation coverage is relatively high, the ratio of form resistance in the total water flow resistance increases with increasing flow rate, and the increased level gradually decreases with an increase in the density. This is possible because the overland water depth gradually increases with an increase in the unit discharge, and the viscous bottom layer is sufficiently thick to cover the roughness factor. As a result, the frictional resistance between the water flow and the underlying surface is reduced, and the grain resistance is lowered. However, under a relatively low degree of vegetation coverage, the blocking effect of the vegetation on the water flow is canceled out by the increase in the flow velocity caused by the vegetation compressing the flow channel. Therefore, the ratio of form resistance exhibits a trend of first increasing and then decreasing. When the vegetation density continues to increase, the probability of friction and collision between the water flow and the vegetation also increases. The increase in the resistance caused by this type of collision will become more obvious as the unit discharge increases. This is because the branches and leaves of the vegetation tend to spread out in space, and the increase in the vegetation's spatial density will increase the vertical contact area between the water flow and the vegetation, thus further slowing the water flow velocity.

4.5. Effects of Vegetation Coverage Change on Surface Runoff

Rujner et al. [47] adopted the rainfall module in MIKE SHE to simulate the hydrological response of grassland irrigation based on the experimental data of 12 irrigation areas. Their results demonstrate the hydraulic conduction and soil conservation benefits of grassland cover. Studies have also shown that changes in vegetation coverage could affect infiltration by changing the volume of runoff [48–50]. As this experiment uses simulated grass under the condition of a certain flow, the influence of vegetation coverage on surface runoff is analyzed by analyzing the residence time of runoff under different coverage degrees.

It can be seen from Table 3 that the residence time of the runoff increases with the coverage rate, which is contrary to the change in the flow velocity. When the coverage rate is less than 47.66%, the change in the residence time is not obvious, and when the vegetation coverage is greater than 47.66%, the change in the residence time becomes larger. For example, when the flow rate is 15 L/min, the coverage rate increases from 0 to 47.66%, and the residence time changes from 13.88 s to 17.73 s. In contrast, when the coverage rate increases from 47.66% to 95.01%, the retention time increases from 17.73 s to 28.43 s. This occurs because when the coverage rate is small, the vegetation has no obvious resistance effect to runoff, and the flow velocity does not change much, causing the residence time to fluctuate only within a small range. With the increase in the coverage rate, the contact area between runoff and vegetation increases significantly. With the increase in the degree of submergence, the frictional resistance also increases, then the pressure difference in the vortex area behind the vegetation in the backwater area after vegetation meets the water surface also increases, and the slow-flow capacity increases significantly, which leads to the extension of the runoff residence time. It can be concluded that changes in the vegetation coverage will increase the soil infiltration time and reduce the runoff kinetic energy, thus regulating runoff. On the other hand, the resistance of the overland flow under vegetation cover can reflect the slow-flow effects of vegetation, and the residence time of the runoff can be analyzed to predict the infiltration condition, which plays a predictive role in soil erosion.

Table 3. Residence time corresponding to different flows under different coverage degrees.

Coverage Degree (%)	Q/(L/min)						
	5	6.4	10	12.5	15	20	30
0	29.65	25.28	17.33	15.23	13.88	12.27	10.07
9.76	31.39	26.98	20.25	20.54	22.09	17.50	12.69
19.97	29.16	25.92	18.52	19.83	20.68	16.44	11.39
38.78	26.73	25.09	18.63	19.38	19.87	15.59	11.91
47.66	28.51	27.28	20.53	18.85	17.73	14.38	12.72
66.42	31.91	30.24	22.92	20.87	19.49	17.78	16.23
76.73	35.96	33.92	24.71	23.52	22.73	20.53	18.33
85.72	38.39	34.88	25.27	25.11	25.00	24.87	20.09
95.01	42.93	37.42	26.24	27.56	28.43	29.52	21.90

4.6. Evaluation and Analysis of Proposed Equation

Figure 13 compares the calculated values of the resistance coefficient from the proposed equations with actual measurements. The closer the *NSE* value is to one, the better is the model-fitting effect. The *NSE* value was determined to be 0.731. Other statistical indicators also show that the simulated value is very close to the measured value (Table 4). Thus, Equation (9) can simulate the resistance coefficient under various degrees of vegetation coverage relatively well. When the resistance coefficient is small, the calculated value of the fitting formula is very close to the measured value; however, when the resistance coefficient is large, some data points have deviated from the 1:1 line. This also reflects the movement pattern of overland flow, which can vary under different degrees of vegetation coverage.

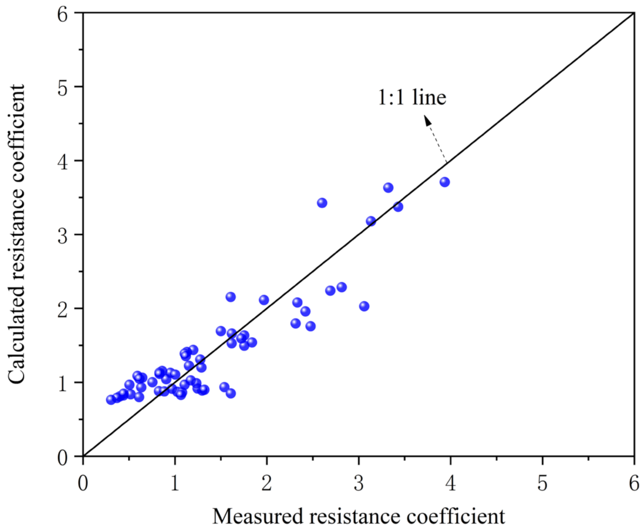

Figure 13. Comparison between the calculated and measured resistance coefficients.

Table 4. Calculation results of different statistical indicators.

Statistical Indicators	*NSE*	R^2	*RMSE*	*MAE*
Calculation results	0.734	0.731	0.344	0.290

5. Conclusions

To explore the influence of vegetation coverage on the hydrodynamic characteristics of overland flow, this study used artificial grass to experimentally simulate the vegetation cover on a slope. Overland flow regime and flow form under the vegetation coverage conditions, as well as the trends in overland flow resistance under the influence of different degrees of vegetation coverage were investigated.

The experimental method developed in this study can accurately control the coverage of simulated vegetation and the rate of flow, which cannot be achieved in many natural conditions. At the same time, many hydraulic parameters obtained from this experiment can provide the basis data for experiments under natural conditions. Normally the particles in the water and the roughness of the underlying surface will change the characteristics of the overland flow; however, the test was conducted under a certain and stable flow rate of the underlying surface, and the infiltration amount and other factors could not be measured. At the same time, owing to the limitation of the experimental data range, the backwater and rolling wave could not be quantitatively analyzed. If the critical water condition of the rolling wave evolution law could be systematically analyzed, it would aid in the mechanism analysis of the attribution of the slope flow pattern. This work will be carried out as the next stage of our research.

Author Contributions: Conceptualization, Z.C.; methodology, Z.C.; software, Z.C., Y.Y. and R.Z.; validation, Z.C. and R.Z.; formal analysis, Z.C.; investigation, Z.C., Y.Y. and R.Z.; resources, Z.C. and R.Z.; data curation, Z.C., Y.Y. and R.Z.; writing—original draft preparation, Z.C.; writing—review and editing, Z.C., Y.Y. and R.Z.; visualization, Z.C., Y.Y. and R.Z.; supervision, J.W.; project administration, J.W.; funding acquisition, J.W. All authors have read and agreed to the published version of the manuscript.

Funding: This research was funded by the National Natural Science Foundation of China, grant number 41771308.

Institutional Review Board Statement: Not applicable.

Informed Consent Statement: Not applicable.

Data Availability Statement: The data that support the findings of this study are available from the corresponding author upon reasonable request.

Conflicts of Interest: The authors declare no conflict of interest.

Appendix A

Calculation of Hydraulic Parameters

The average flow velocity u of the sections was calculated using the continuity equation, as follows:

$$u = \frac{Q}{Bh} \tag{A1}$$

where Q is the flow rate, in m^3/s; B is the flume width (0.3 m in this test); and h is the average water depth of the sections, in m.

The hydraulic binary flow Reynolds number Re was used to determine the flow regime of the water flow using the following formula:

$$Re = \frac{uR}{v} \tag{A2}$$

where R is the hydraulic radius, in m; the sheet flow can be considered to be a binary flow; the water depth h can be used to replace R; and v is the kinematic viscosity coefficient, in m^3/s, which can be calculated using the Poiseuille formula as follows:

$$v = \frac{0.01775}{1 + 0.0337t + 0.000221t^2} \tag{A3}$$

where t is the water temperature, in °C. The water temperature was recorded using a thermometer; it has an accuracy of 0.1 °C.

The formula for the Froude number is as follows:

$$Fr = \frac{u}{\omega} \tag{A4}$$

where ω is the speed of the microwave:

$$\omega = \sqrt{\frac{gh(1 + \Delta h)^2}{1 + \frac{0.5\Delta h}{h}}} \tag{A5}$$

Here, Δh is the height of the rolling wave, in m, and g is the acceleration of gravity ($9.81\ m/s^2$).

In this experiment, the Darcy–Weisbach formula was used to calculate the resistance coefficient λ for each test group:

$$\lambda = \frac{8gRJ}{u^2} \tag{A6}$$

where J is the hydraulic slope gradient (taken as $J = \sin\theta$ in the laboratory).

References

1. Fu, B.; Wang, S.; Liu, Y.; Liu, J.; Liang, W.; Miao, C. Hydrogeomorphic ecosystem responses to natural and anthropogenic changes in the Loess Plateau of China. *Annu. Rev. Earth Planet. Sci.* **2017**, *45*, 223–243. [CrossRef]
2. Sun, W.; Shao, Q.; Liu, J. Soil erosion and its response to the changes of precipitation and vegetation coverage on the Loess Plateau. *J. Geogr. Sci.* **2013**, *23*, 1091–1106. [CrossRef]
3. Chen, Y.; Wang, K.; Lin, Y.; Shi, W.; Song, Y.; He, X. Balancing green and grain trade. *Nat. Geosci.* **2015**, *8*, 739–741. [CrossRef]
4. Zhang, K.D.; Wang, G.Q.; Sun, X.M.; Wang, J.J. Hydraulic characteristic of overland flow under different vegetation coverage. *Adv. Water Sci.* **2014**, *25*, 825–834.
5. Zhao, C.H.; Gao, J.E.; Zhang, M.J.; Wang, F.; Zhang, T. Sediment deposition and overland flow hydraulics in simulated vegetative filter strips under varying vegetation covers. *Hydrol. Process.* **2016**, *30*, 163–175. [CrossRef]

6. Srivastava, A.; Kumari, N.; Maza, M. Hydrological response to agricultural land use heterogeneity using variable infiltration capacity model. *Water Resour. Manag.* **2020**, *34*, 3779–3794. [CrossRef]
7. Li, M.; Yao, W.Y.; Li, Z.B. Progress of the effect of grassland vegetation for conserving soil and water on loess plateau. *Adv. Earth Sci.* **2005**, *20*, 74–80.
8. Foster, G.R.; Huggins, L.F.; Meyer, L.D. A laboratory study of rill hydraulics: I. Velocity relationships. *Trans. ASAE* **1984**, *27*, 790–796. [CrossRef]
9. Foster, G.R.; Huggins, L.F.; Meyer, L.D. A Laboratory Study of Rill Hydraulics: II. Shear Stress Relationships. *Trans. ASAE* **1984**, *27*, 797–804. [CrossRef]
10. Abrahams, A.D.; Li, G.; Parsons, A.J. Rill hydraulics on a semiarid hillslope, southern Arizona. *Earth Surf. Process. Landf.* **1996**, *21*, 35–47. [CrossRef]
11. Selby, M.J. *Hillslope Materials and Processes*; Oxford University Press: Oxford, UK, 1993.
12. Pute, W.; Peihua, Z. Research on the laminar flow type and erosion transportation manners on the slope surface. *J. Soil Water. Conserv.* **1992**, *6*, 16–24.
13. Horton, R.E. Erosional development of streams and their drainage basins; Hydrophysical approach to quantitative morphology. *Geol. Soc. Am. Bull.* **1945**, *56*, 275–370. [CrossRef]
14. Zhang, G. Study on hydraulic properties of shallow flow. *Adv. Water Sci.* **2002**, *13*, 159–165.
15. Wu, Q.; Wu, F.; Wang, L. Hydrodynamic characteristics of overland flow under soil crusts condition. *Trans. Chin. Soc. Agric. Eng.* **2014**, *30*, 73–80.
16. Pan, C.Z.; Shangguan, Z.P. Runoff hydraulic characteristics and sediment generation in sloped grassplots under simulated rainfall conditions. *J. Hydrol.* **2006**, *331*, 178–185. [CrossRef]
17. Cao, Y.; Zhang, G.H.; Tang, K.M.; Luo, R. Experiment on the effect of simulated surface cover on the overland flow velocity. *J. Mt. Sci.* **2011**, *29*, 654–659.
18. Järvelä, J. Flow resistance of flexible and stiff vegetation: A flume study with natural plants. *J. Hydrol.* **2002**, *269*, 44–54. [CrossRef]
19. Ling, H.; Guo, B.; Xu, H.; Fu, J. Configuration of water resources for a typical river basin in an arid region of China based on the ecological water requirements (EWRs) of desert riparian vegetation. *Glob. Planet. Change* **2014**, *122*, 292–304. [CrossRef]
20. Jiang, C.B.; Long, Y.N.; Hu, S.X.; Peng, Y.P. Recent progress in studies of overland flow resistance. *J. Hydraul. Eng.* **2012**, *43*, 189–197.
21. Zhang, K.; Wang, Z.; Wang, G.; Sun, X.; Cui, N. Overland-flow resistance characteristics of nonsubmerged vegetation. *J. Irrig. Drain. Eng.* **2017**, *143*, 04017021. [CrossRef]
22. Smith, M.W. Applying flow resistance equations to overland flows. *Prog. Phys. Geogr.* **2007**, *31*, 363–387. [CrossRef]
23. Ogunlela, A.O.; Makanjuola, M.B. Hydraulic roughness of some African grasses. *J. Agric. Eng. Res.* **2000**, *75*, 221–224. [CrossRef]
24. Wang, P.-F.; Wang, C.; Zhu, D.Z. Hydraulic resistance of submerged vegetation related to effective height. *J. Hydrodyn. Ser. B* **2010**, *22*, 265–273. [CrossRef]
25. Chen, G.X.; Yao, W.Y. Effect of rainfall on hydraulic resistance of shallow flow. *Adv. Water Sci.* **1996**, *7*, 42–46.
26. Noarayanan, L.; Murali, K.; Sundar, V. Performance of flexible emergent vegetation in staggered configuration as a mitigation for extreme coastal disasters. *Nat. Hazards* **2012**, *62*, 531–550. [CrossRef]
27. Li, G. Preliminary study of the interference of surface objects and rainfall in overland flow resistance. *Catena* **2009**, *78*, 154–158. [CrossRef]
28. Blöschl, G.; Bierkens, M.F.P.; Chambel, A.; Cudennec, C.; Destouni, G.; Fiori, A.; Kirchner, J.W.; McDonnell, J.J.; Savenije, H.H.G.; Sivapalan, M.; et al. Twenty-three unsolved problems in hydrology(UPH)-A community perspective. *Hydrol Sci. J.* **2019**, *64*, 1141–1158. [CrossRef]
29. Paniconi, C.; Putti, M. Physically based modeling in catchment hydrology at 50: Survey and outlook. *Water Resour. Res.* **2015**, *51*, 7090–7129. [CrossRef]
30. Paul, P.K.; Kumari, N.; Panigrahi, N.; Mishra, A.; Singh, R. Implementation of cell-to-cell routing scheme in a large scale conceptual hydrological model. *Environ. Modell. Softw.* **2018**, *101*, 23–33. [CrossRef]
31. Che, T.; Li, X.; Liu, S.; Li, H.; Xu, J.; Tan, J.; Zhang, Y.; Ren, Z.; Xiao, L.; Jin, R.; et al. Integrated hydrometeorological, snow and frozen-ground observations in the alpine region of the Heihe River Basin, China. *Earth Syst. Sci. Data* **2019**, *11*, 1483–1499. [CrossRef]
32. Cheng, G.; Li, X.; Zhao, W.; Xu, Z.; Feng, Q.; Xiao, S.; Xiao, H. Integrated study of the water-ecosystem-economy in the Heihe River Basin. *Natl. Sci. Rev.* **2014**, *1*, 413–428. [CrossRef]
33. Pan, C.Z.; Shangguan, Z.P. Experimental study on influence of rainfall and slope gradient on overland shallow flow hydraulics. *J. Basic Sci. Eng.* **2009**, *17*, 843–851.
34. Jiao, J.Y.; Wang, W.Z. Non-uniformity of spatial distribution of rainfall on the Loess Plateau. *Hydrology* **2001**, *2*, 20–24.
35. Zhang, K.D.; Wang, G.Q.; Lv, H.X.; Wang, Z.L. Discussion on flow pattern determination method of shallow flow on the slope surface. *J. Exp. Fluid Mech.* **2011**, *25*, 67–73.
36. Rauws, G. Laboratory experiments on resistance to overland flow due to composite roughness. *J. Hydrol.* **1988**, *103*, 37–52. [CrossRef]
37. Zhao, C.H.; Gao, J.E.; Huang, Y.; Wang, G.; Zhang, M. Effects of vegetation stems on hydraulics of overland flow under varying water discharges. *Land Degrad. Dev.* **2016**, *27*, 748–757. [CrossRef]

38. Yan, X.F.; Zhou, S.F.; Huang, E.; Liu, X.N.; Wang, X.K. Experimental study on the effects of vegetation on hydraulic characteristics of overland flow. *J. Sichuan Univ. Eng. Sci. Edit.* **2012**, *44*, 26–30.
39. Lawrence, D.S.L. Macroscale surface roughness and frictional resistance in overland flow. *Earth Surf. Process. Landf.* **1997**, *22*, 365–382. [CrossRef]
40. Zhang, G.; Liu, G.; Yi, L.; Zhang, P. Effects of patterned Artemisia capillaries on overland flow resistance under varied rainfall intensities in the Loess Plateau of China. *J. Hydrol. Hydromech.* **2014**, *62*, 334–342. [CrossRef]
41. Wu, F.-C.; Shen, H.W.; Chou, Y.-J. Variation of Roughness Coefficients for Unsubmerged and Submerged Vegetation. *J. Hydraul. Eng.* **1999**, *125*, 934–942. [CrossRef]
42. Ishikawa, Y.; Mizuhara, K.; Ashida, S. Effect of density of trees on drag exerted on trees in river channels. *J. For. Res.* **2000**, *5*, 271–279. [CrossRef]
43. Tanino, Y.; Nepf, H.M. Laboratory investigation of mean drag in a random array of rigid, emergent cylinders. *J. Hydraul. Eng.* **2008**, *134*, 34–41. [CrossRef]
44. Dunkerley, D.; Domelow, P.; Tooth, D. Frictional retardation of laminar flow by plant litter and surface stones on dryland surfaces: A laboratory study. *Water Resour. Res.* **2001**, *37*, 1417–1423. [CrossRef]
45. Yi, L.; Ming'an, S. Hydro-dynamic parameters of overland flow during laboratory rainfall experiments under grass coverage. *Trans. Chin. Soc. Agric. Eng.* **2008**, *10*, 1–5.
46. Wu, S.F.; Wu, P.T.; Feng, H.; Li, M. Effects of forage grass on the reduction of runoff and sediment and the hydrodynamic characteristic mechanism of slope runoff in the standard slope plot. *J. Beijing For. Univ.* **2007**, *29*, 99–104.
47. Rujner, H.; Leonhardt, G.; Marsalek, J. High-resolution modelling of the grass swale response to runoff inflows with Mike SHE. *J. Hydrol.* **2018**, *562*, 411–422. [CrossRef]
48. Guo, J.K.; Yu, B.Q.; Zhang, Y.; Che, S. Predicted models for potential canopy rainfall interception capacity of landscape trees in Shanghai, China. *Eur. J. Forest. Res.* **2017**, *136*, 387–400. [CrossRef]
49. Espeland, E.K.; Emery, N.C.; Mercer, K.L.; Woolbright, S.A.; Kettenring, K.M.; Gepts, P.; Etterson, J.R. Evolution of plant materials for ecological restoration: Insights from the applied and basic literature. *J. Appl. Ecol.* **2017**, *54*, 102–115. [CrossRef]
50. Sun, X.P.; Zhang, Y.L.; Shen, Y.; Randhir, T.O. Exploring ecosystem services and scenario simulation in the headwaters of Qiantang River watershed of China. *Environ. Sci. Pollut. Res.* **2019**, *26*, 1–19. [CrossRef]